The Box H/ACA snoRNP Assembly Factor Shq1p is a Chaperone Protein Homologous to Hsp90 Cochaperones that Binds to the Cbf5p Enzyme

Katherine Godin, Hélène Walbott, Nicolas Leulliot, Herman van Tilbeurgh, Gabriele Varani

Published in final edited form as:
J Mol Biol. 2009 July 10; 390(2): 231–244. doi:10.1016/j.jmb.2009.04.076.

The Box H/ACA snoRNP assembly factor Shq1p is a chaperone protein homologous to Hsp90 co-chaperones that binds to the Cbf5p enzyme

Katherine S. Godin[1], **Hélène Walbott**[2], **Nicolas Leulliot**[2,3], **Herman van Tilbeurgh**[2], and **Gabriele Varani**[1,4,§]

[1] Department of Chemistry, Box 351700, University of Washington, Seattle, Washington 98195

[2] Institut de Biochimie et Biophysique Moléculaire et Cellulaire, Université Paris-Sud 11, 91400 Orsay, France

[3] Laboratoire de Cristallographie et RMN Biologiques, Université Paris Descartes, CNRS, 4 Avenue de l'Observatoire, 75006 Paris, France

[4] Department of Biochemistry, Box 357350, University of Washington, Seattle, Washington 98195

Abstract

Box H/ACA small nucleolar ribonucleoproteins (snoRNPs) are responsible for the formation of pseudouridine in a variety of RNAs, and are essential for ribosome biogenesis, modification of spliceosomal RNAs and telomerase stability. The mature snoRNP has been reconstituted *in vitro* and is composed of a single RNA and four proteins. However, snoRNP biogenesis *in vivo* requires multiple factors to coordinate a complex and poorly understood assembly and maturation process. Among the factors required for snoRNP biogenesis in yeast is Shq1p, an essential protein necessary for the snoRNA stable expression. We have found that Shq1p consists of two independent domains that contain Casein Kinase 1 phosphorylation sites. We also demonstrate that Shq1p binds the pseudourydilating enzyme Cbf5p through the C-terminal domain in synergy with the N-terminal domain. The NMR solution structure of the N-terminal domain has striking homology to the 'Chord and Sgt1' (CS) domain of known Hsp90 co-chaperones, yet Shq1p does not interact with the yeast Hsp90 homologue *in vitro*. Surprisingly, Shq1p has stand-alone chaperone activity *in vitro*. This activity is harbored by the C-terminal domain but it is increased by the presence of the N-terminal domain. These results provide the first evidence of a specific biochemical activity for Shq1p and a direct link to the H/ACA snoRNP.

Keywords

H/ACA snoRNP biogenesis; Shq1; CS domain; chaperone

§To whom correspondence should be addressed: tel 206.543.7113; fax 206 685 8665; email varani@chem.washington.edu.

Introduction

Box H/ACA small nucleolar (sno)RNAs are a class of non-coding RNA that play a fundamental role in ribosome biogenesis, spliceosome assembly, and telomere maintenance (for review see [1] and [2]). In mammals, each of the ~100 H/ACA snoRNAs combines with four highly conserved protein components to form enzymatically active small nucleolar ribonucleoproteins (snoRNPs): the Cbf5p catalytic subunit (dyskerin in humans or NAP57 in rodents), Nop10p, Nhp2p (L7Ae in archaea), and Gar1p. These enzymes primarily function in the nucleolus to catalyze site-specific pseudouridylation of pre-ribosomal (pre-r)RNA[3, 4], but a fraction modify small nuclear (sn)RNPs when directed to Cajal bodies by Cajal body specific (sca)RNAs[5, 6]. Some H/ACA snoRNPs do not have pseudouridylase activity, including yeast snR30 (E1/U17 in vertebrates) that participates in pre-rRNA cleaveage[7, 8] and the telomerase H/ACA scaRNA motif[9] that is essential *in vivo* for proper RNA processing, activity, and nucleolar localization[10, 11, 12].

The macromolecular architecture and the enzymatic role of each protein have been studied with *in vitro* reconstituted archaeal small (s)RNPs, consisting of a single hairpin small (s)RNA and the four evolutionarily conserved protein homologues (for review see [13]). However, in eukaryotes, H/ACA snoRNP biogenesis pathway is surprisingly complex requiring several more proteins than are present in the mature functional holoenzyme (for review see [14]). Assembly of the mature proteins follows a coordinated stepwise process requiring the formation and disassembly of intermediate structures within specific sub-nuclear compartments[15, 16]. Stable expression of H/ACA snoRNAs requires the co-transcriptional formation of an inactive RNP by the association of Cbf5p, Nop10p, Nhp2p, and the H/ACA assembly factor Naf1p[17, 18]. Gar1 is not found at the transcription site with the other snoRNP proteins but is concentrated in the nucleolus[19] and within Cajal bodies[20]; this protein likely associates with the RNP late in the maturation process. Cbf5p mediates the interaction of Naf1p with the other snoRNP proteins during snoRNA transcription[15, 17, 18], yet Naf1p does not localize with the other snoRNP proteins to the nucleolus or Cajal bodies. Since the specificity of Naf1p for the H/ACA snoRNP arises from its Gar1-like domain[21], which makes it interact with Cbf5p in a manner that is competitive with Gar1, the snoRNP is presumed to undergo a remodeling event to introduce Gar1 and form mature functional snoRNP particles.

A second eukaryotic H/ACA snoRNP assembly factor, Shq1, was found to associate with Naf1p in proteomic, *in vitro* pull-down, and co-localization studies[22]. Genetic depletion of Shq1p results in ribosomal RNA processing defects due to the loss of stable accumulation of H/ACA snoRNAs. Shq1p was also found to associate with *in vitro* translated Nhp2p[22] and flag-tagged Cbf5[23], providing an additional and direct link to H/ACA snoRNPs biogenesis. Since levels of Nhp2p protein are unaffected in Shq1p depleted cells, Shq1p probably functions directly in the maturation of H/ACA snoRNPs.

Sequence analysis indicates that Shq1p has two structural domains. We show that these two domains do not interact with each other, yet the interaction between Shq1p and Cbf5, that we report here, requires both domains. We report the solution structure of its N-terminal domain which shows that it adopts a ‘Chord and Sgt1’ (CS) fold related to the Hsp90 co-chaperones Sgt1 and Sba1p/p23 proteins but, as recently reported, this domain does not interact directly with the yeast Hsp90 homologue[24]. We further show that the C-terminal domain does not rescue binding of Shq1p to Hsp90. However, we report that the C-terminal domain has stand-alone chaperone-like activity that is enhanced in the complete protein. We also observe that both domains of Shq1p are substrates for Casein Kinase 1 (CK1) phosphorylation.

Results

Shq1p has two structurally independent domains

Yeast Shq1p consists of 507 residues with very high sequence conservation from yeast to humans (Figure 1). Comparison of Shq1p with sequences from known domains or motifs using the interpro database[25] suggests that Shq1p contains two domains, a CS domain within the first 100 residues and a C-terminal sequence unique to Shq1. To verify this assumption, purified wild type Shq1p was digested three different ways with proteinase K, trypsin, or chymotrypsin. Analysis by SDS-PAGE consistently showed the presence of a small ~12kDa product and a larger fragment that ranged in size from ~30–45kDa. Gel filtration revealed that the two domains eluted as independent entities at the appropriate molecular weight identified from SDS-PAGE (data not shown), suggesting that the two domains do not interact with each other strongly or self-aggregate.

The N-terminal construct Shq1Np (Figure 1B) identified from partial proteolysis ranges from residue I2 to N132 (~15kDa). It gave uniform peak shapes and dispersion in a ^{15}N-HSQC spectrum (Figure 2A), indicative of a well-folded protein. A ^{15}N-HSQC of the full length Shq1p contained all resonances of the Shq1Np fragment with chemical shifts consistent with the individually purified N-terminal domain (Figure 2B), supporting the conclusion that the N-terminal domain does not associate with the larger C-terminal domain. Altered chemical shifts were observed for S27, G30, T64, K80, D89–L92, A98, and the amines of Q10 and N75.

Shq1p interacts with Cbf5

To establish if and how Shq1p associates with H/ACA protein components during snoRNP biogenesis, we analyzed the interaction of each of its domains with snoRNP components. Earlier studies showed that Shq1p is essential for snoRNA accumulation and it was initially reported to interact with Naf1p and Nhp2p[22]. However, we observed no interaction with the Gar1-domain of Naf1p by pull-down assays or even by NMR (data not shown), confirming the results obtained using Tap-tag pull-downs of Naf1p which failed to retrieve Shq1p[18]. We found instead that full-length Shq1p was pulled down efficiently by refolded His-tagged Cbf5$^{\Delta}$p (Figure 2C, lane 2) confirming previous observations that Shq1p co-purifies with over-expressed flag-tagged Cbf5[23] and consistent with recent studies of mammalian SHQ1[26]. In addition, Shq1Cp appears to be weakly associated with Cbf5$^{\Delta}$p, but Shq1Np does not interact with Cbf5p at all (Figure 2C, lane 3 and 4). These results support a role for both domains of Shq1p in Cbf5p recognition, but reveal a prominent role for the C-terminal domain.

The Shq1p N-terminus is structurally homologous to Hsp90 co-chaperones

The structure of the putative CS domain of Shq1Np (PDB 2K8V) was determined by NMR using methods described below and calculated with CYANA 2.1 based on 4521 NOEs selected from ^{15}N-edited NOESY, ^{13}C-edited NOESY, and ^{1}H,^{1}H-NOESY, as well as additional dihedral angle and hydrogen bond constraints generated from the NMR data as described. In the early rounds of CYANA, each assignment was validated by a network NOEs arising from neighboring residues and residues that satisfy the tertiary fold. The NOE assignments were used to derive a total of 2621 meaningful upper distance limits (~20 constraints/residue) in the last round of refinement and produced 20 structures with the lowest violations, the best overall statistics (Table 1) and excellent structural convergence (Figure 3A). The high quality is reflected in the tight convergence of the 20 structures with the respective average backbone and heavy atom r.m.s.d. to the mean of 0.25Å and 0.71Å over the structured region and the very favorable Ramachandran statistics. The exceptional structural statistics and strong validation of the predicted CS domain fold (discussed below) indicated that the CYANA solution was correct and additional refinement using Residual Dipolar Coupling was not necessary.

Shq1Np contains 7 β-strands and a small α-helix kinked by a single proline residue that packs into a compact two-layer β-sandwich (Figure 3B), as in the recently-reported crystal structure of the same domain[24]. This topology is consistent with known CS domain proteins Sgt1, Sba1p/p23, and Siah-interacting protein (SIP) where the larger β-sheet contains 4 antiparallel strands β1, β2, β6, and β7 and the smaller has 3 anti-parallel strands β3, β4, and β5. The two sheets pack against each other through a vast network of hydrophobic side chains. The hydrophobic core accommodates 7 aromatic residues, all of which are very highly conserved and tightly packed against the abundant aliphatic side chains that anchor the β-strands within each β-sheet and across the sandwich interior.

The NMR structure superposes very well with the crystal structure (3EUD, 1.26 Å r.m.s.d), with only small differences in the conformation of the β2–β3 loop which is involved in crystal packing[24]. In solution, residues 100–134 are disordered, confirming that the structural core of the N-terminal domain encompasses residues 1–100, corresponding to the crystallized fragment. A search on the DALI server[27] retrieved the expected structural homologues of Shq1p within the CS domain family proteins Sgt1 (1RL1, 7.8 Z-score, 1.9Å r.m.s.d), p23 (yeast Sba1) (1EJF, 7.8 Z-score, 2.2Å r.m.s.d.), and Siah-interacting protein (1X5M, 7.6 Z-score, 2.6Å r.m.s.d.). More distant similarities were found with several small heat shock protein-like (sHsp-like) chaperones with the predominant α-crystallin fold Hsp26 (2H53, 6.8 Z-score, 1.9Å r.m.s.d), Hsp16.9B (1GME, 6.8 Z-score, 2.2Å r.m.s.d), and *M. jannaschii* sHsp (1SHS, 7.1 Z-score, 2.2Å r.m.s.d). In comparison to CS domain proteins, Hsp20 chaperones have an extended β4–β5 loop that facilitates dimerization by domain swapping[28]; in the CS domain proteins this loop is considerably shorter; the shortest so far is found in Shq1Np.

The edges of the sandwich are sealed on three of the four sides forming a robust and compact globular structure. Hydrogen bonded amides remained observable in ^2H_2O for at least four months and at temperatures of up to 55°C. Several residues located within loops between β-strands 1–2, 3–4, 4–5, and from strand β7 to the α-helix showed protection from exchange as well, suggesting that the loops are rigid and highly ordered. The lack of hydrogen bond restraints along strands β3 and β6 suggests instead that this region is solvent exposed and corresponds to a noticeable crevice that is not observed in either Sba1p/p23 or Sgt1. This pocket is unique to Shq1Np and forms as a result of the lack of hydrophobic packing between the shorter internal Ser and Ala side chains of β6 and the larger hydrophobic residues of β3. Analysis of the crystal packing of the crystal structure of Shq1p shows that this pocket is always involved in protein-protein interactions[24]. Of notice is also Lys80, a strictly conserved residue which assumes an unusual position for a charged residue, being deeply buried within the hydrophobic core. Mutation of this residue has been shown to be lead to severe growth defects in yeast[24].

Shq1p does not interact directly with Hsp90

The CS domains of both Sba1p/p23 and Sgt1 interact with the ubiquitous macromolecular chaperone Hsp90[29, 30]. Both proteins share the CS domain fold and have been shown in x-ray crystallographic structures to interact with Hsp90 in very distinct ways[31, 32, 33]. The Hsp90 binding interface of both Sba1p/p23 and Sgt1 overlap with the regions displaying the most highly conserved surface exposed residues found along different faces of each CS domain. The Sba1p/p23-Hsp90 interface includes several residues from the unique C-terminal β8 strand and wraps around the β5-β8-β1 edge of Sba1p/p23 to the surface exposed residues found in the β2–β3 loop and β6–β7 loop along the lower face of the large 4 stranded β-sheet (Figure 4A) [31]. This protein interacts with the amino terminus of ATP-bound Hsp90 constraining features important for ATP turnover and, as a result, regulates the rate of ATP hydrolysis and stabilizes this bound state for chaperone activity. The Sgt1 CS domain recently crystallized with Hsp90 shows a distinct mode of interaction with the Hsp90 N-terminus. Sgt1 utilizes highly conserved

residues found on the first 3 strands of the large β-sheet belonging to its CS domain (Figure 4B) but does not interact with features of Hsp90 important for ATP hydrolysis[32, 33]. Unlike Sba1p/p23, Sgt1 does not require ATP to interact with Hsp90[34], but appears to behave instead as an adaptor that links Hsp90, through its CS domain, to other client proteins[35, 36, 37].

The structural homology of Shq1p with CS domain proteins obviously suggests that Shq1p is also an Hsp90 co-chaperone. Highly conserved residues on the Shq1Np surface appear along the β5-α1-β1 face and within the β2–β3 loop that corresponds to the Sba1p/p23 Hps90-interface (Figure 4A and B). When comparing the surface electrostatic potentials, we observe that Shq1Np also shares a similar electrostatic distribution with the Hsp90 binding face of Sba1p/p23 (Figure 4A), suggesting that Shq1Np could interact with Hsp90 in a similar way to what has been seen in the Sba1p/p23-Hsp90 complex. However, surface exposed residues along the Sba1/p23 face important for Hsp90 recognition are not found with the same Shq1Np surface.

In order to establish whether the CS domain of Shq1p is capable of interacting with Hsp90 *in vitro*, we expressed and purified full length Hsp82p (the yeast Hsp90 homologue). As recently reported[24, 26], we observed no interaction between Hsp82p and the N-terminal Shq1p domain by NMR, pull-down assay or gel filtration, both in the presence or absence of ATP or ATP analogs. Reasoning that perhaps binding surfaces on either protein could be masked in the full proteins and only exposed by some unknown regulatory event, we also independently expressed the N-terminal, middle, and C-terminal domains of Hsp82p. We then probed for the interaction with Shq1p of each of these three constructs independently, but also failed to observe any interaction (data not shown). Since we have shown that Shq1p interacts with Cbf5p prominently through the C-terminal domain, and that the N-terminal domain does not bind Cbf5p by itself, we also probed the interaction of Hsp82p with full-length Shq1p and the separate Shq1p N- and C-terminal domains. As can be seen in Figure 4C, no interaction could be observe between Hsp82p and the complete full length Shq1p or even with the separate Shq1Np or Shq1Cp domain by pull-down assays or gel filtration, both in the presence or absence of ATP or ATP analogs. These results conclusively demonstrate that neither the N- or C-terminal domains of Shq1p are capable of binding Hsp82p *in vitro*.

Shq1p is phosphorylated by Casein Kinase I

While testing the interaction between Shq1Np and Hsp90 by NMR, we observed small chemical shift changes of Shq1Np residues in the presence of ATP (data not shown). These changes are not indicative of specific ATP binding since the same changes were observed with GTP and were not observed in the absence of Mg^{2+} counter ions. Additionally we could not identify any ATP binding when using electrospray ionization mass spectrometry or radioactive binding assays (data not shown). However, these chemical shift changes drew our attention to two deep pockets located on the β3–β6 face and the pocket generated by Leu44 extending from the β4–β5 loop to Phe26 (Figure 5A). These two pockets are not found in either Sba1p/p23 or Sgt1 that have longer β4–β5 loops and where the β3–β6 face is filled by aromatic residues on both β-strands. Interestingly, residual electron density in the pocket located on the β3–β6 face in one of the molecules of the asymmetric unit of the crystal structure of Shq1p[24] reveals an unidentified bound small molecule.

The pockets contain three Serines, Ser27, Ser45 and Ser63; interestingly, the Ser63 hydroxyl group is within ~3Å of the Asp59 acetate, suggestive of a catalytically active site that may facilitate abstraction of the hydrogen from the Serine hydroxyl. We hypothesized that the serines within these pockets are substrates for post-translation phosphorylation but did not observe autophosphorylation upon incubation of Shq1Np or Shq1FLp with ^{32}P-[γ]ATP (data not shown). Consistent with this suggestion, KinasePhos[38] predicts that Ser63, found within the consensus sequence (D/E/SpXXS) for Casein Kinase 1 (CK1) phosphorylation, is a potential phosphorylation site. CK1 plays an important role in many diverse cellular activities

by phosphorylating regulatory proteins that participate in membrane transport, cell division, DNA repair, circadian rhythms, and nuclear localization (for review see [39]). Using the CK1εorδ isoform of this kinase, we observed transfer of the ^{32}P-[γ]ATP γ-phosphate group to the R3 region of APC (adenomatis polyposis coli), a protein that facilitates nuclear export of β-catenin and is hyperphosphorylated by CK1[40], as a positive control for kinase activity. We observed that CK1 phosphorylates each construct of Shq1p indicating that Shq1p is indeed a CK1 substrate (Figure 5B). The CK1 phosphorylation site within the Shq1p C-terminal domain is predicted by KinasePhos to reside at Ser462. Rna15 from yeast, a protein involved in processing RNAPII transcription products[41], was not predicted to be a CK1 substrate by KinasePhos nor is it known as phosphoprotein. As expected, Rna15p was not phosphorylated in a negative control experiment, demonstrating that Shq1Np is a *bona fide* substrate of CK1.

Since CK1 is known to be a promiscuous enzyme[42] *in vitro*, its specificity for Ser63 was tested by generating a Ser63Ala point mutation of the Shq1Np construct. However, phosphorylation of Shq1Np-S63A by CK1 remained unchanged; we reasoned that the specific activity of CK1 on Ser63 may be masked by non-specific phosphorylation of residues in the C-terminal tail of the protein. Consistent with this hypothesis, truncation of both Shq1Np constructs to residue Gly101 (Shq1Np-101wt and Shq1Np-101S63A) greatly reduced the extent of phosphorylation by CK1 and showed a significant decrease in the phosphorylation of the Ser63Ala mutant as well (Figure 5C). Residual phosphorylation of Shq1Np-101S63A is likely due to additional non-specific activity of CK1. Kinases that were not predicted by KinasePhos, Protein Kinase A (PKA) and Casein Kinase II (CK2), were incubated with Shq1Np-101 overnight and were unable to induce significant phosphorylation (Figure 5D). These results suggest that Shq1p is a specific target for CK1 directed phosphorylation and that these post-translation modifications may regulate its activity or protein-protein interactions.

Shq1p has general chaperone activity

Surprised by the lack of interaction between Shq1Np and Hsp90, we performed a classical assay to test general chaperone activity in an attempt to assign a molecular function to Shq1p. The assay involves monitoring thermal aggregation of citrate synthase by light scattering[43]. The addition of a general molecular chaperone, such as p23, has been shown to prevent aggregation of citrate synthase and thus to reduce light scattering[44, 45].

Thermal aggregation of citrate synthase was observed during incubation at 45°C, as expected (Figure 6). A concentration-dependent decrease in light scattering was observed and full length Shq1p was very efficient at suppressing citrate synthase aggregation at 1:1 molar ratio (Figure 6A). Citrate synthase aggregation was also strongly inhibited by the presence of Shq1Cp (over 50% of light scattering reduction at a ratio of 1:1), whereas Shq1Np had no effect (Figure 6B). A mix of Shq1Np and Shq1Cp had the same activity as Shq1Cp alone, showing that the N-terminal domain of Shq1p increases the chaperone activity only when it is present in the same polypeptide chain. In a negative control experiment, an equimolar ratio of BSA did not affect the thermal aggregation behaviour of citrate synthase (Figure 6A). In further control experiments, we verified that Shq1FL, Shq1Np, and Shq1Cp were not susceptible to aggregation under these conditions and that the addition of ATP did not have a significant impact on activity (data not shown). Thus, Shq1p has a stand-alone general chaperone activity provided by its C-terminal domain but reinforced by its N-terminal CS domain.

Discussion

Stable accumulation of mature H/ACA snoRNAs in eukaryotes requires co-transcriptional association with protein factors that protect the snoRNA from degradation and promote the step-wise assembly of the mature RNP[15, 17, 18]. This assembly process is assisted by at least two proteins that appear to be specific for this class of snoRNPs, Naf1p and Shq1p[22]. A direct

role for Naf1p recruitment to Cbf5p during snoRNA transcription and exchange with Gar1p at later stages of the maturation process was demonstrated[15, 17, 18]. Here we show that Shq1p is composed of two structurally independent domains that contain phosphorylation sites, harbor protein chaperone activity and bind to Cbf5p directly. Consistent with this result, while preparing this manuscript, mammalian SHQ1 was reported to interact with NAP57 specifically through its C-terminal domain and prior to the association of NAF1 and other H/ACA snoRNP proteins[49]. Although these new findings contradict the initial yeast two-hybrid and genetic depletion experiments that suggested a direct association with Naf1p, they are in agreement with our biochemical analysis. We confirm and extend recent results showing that Shq1p does not interact directly with Hsp82p[24, 26], the yeast Hsp90 homologue, although the N-terminus of Shq1p has strong sequence and structural homology to the CS domains of Hsp90 co-chaperones. Our solution structure of Shq1N is consistent with the x-ray crystal structure[24] and other CS domain proteins; we have further expanded this analysis by including deuterium exchange experiments, relaxation measurements, and radioactive phosphorylation assays to propose a functional role for Shq1p.

Genetic depletion and co-immuno precipitation from mammalian cell extracts[46], as well as cell viability studies and snoRNA microarrays in yeast[47], have shown that the chaperone Hsp90 and the R2TP complex are generally important for the biogenesis of RNPs containing L7Ae homologs, These RNPs include the H/ACA snoRNPs and a second related class responsible for 2′O-methylation known as the C/D snoRNPs. A direct association between Cbf5p and Hsp90 has also been observed *in vivo* using TAP tag pull-downs[48, 49], supporting a role for the chaperone activity of Hsp90 in Box H/ACA biogenesis. Consistent with a role for Shq1p in Hsp82p recruitment, the integrity of the Sba1p/p23-Hsp90-like interface of Shq1p was recently shown to be important *in vitro* and *in vivo* for protein stability and snoRNA processing[24]; yet, we and others[24] have independently failed to observe any direct interaction between this domain of Shq1p and Hsp82p *in vitro*. Reasoning that the Hsp82p-Shq1p interaction may be auto-inhibited in the full-length proteins, we also tested multiple domain constructs of each protein, but still failed to observe any interaction even at the concentrations required for NMR. Shq1Np is structurally distinct from Sgt1 and Sba1p/p23 because of the presence of a C-terminal α-helix tightly bound to strands β1 and β5, the shorter β4–β5 loop that forms a small surface pocket as well as the proposed Ser63 phosphorylation pocket. Interestingly, these two regions contained residues whose chemical shifts are altered when in the full length protein. Thus, it remains formally possible that Shq1p interacts with Hsp82p only when it is in a defined conformation or when bound to another protein cofactor yet to be discovered.

Although the presence of ATP did not reverse the negative results of our *in vitro* binding studies, as was hoped, it nonetheless brought attention to two deep surface pockets containing potential phosphorylation substrates. The deep pocket between strands β3 and β6 contains a canonical Casein kinase 1 (CK1) recognition motif suggesting that Ser63 is a phosphorylation target[39, 40]. This loop is also the most solvent-exposed region within the structure, suggesting that it may be easily accessible for kinase modification. Indeed we observed that CK1 readily phosphorylates the N- as well as C-terminal domain of Shq1p. The region of Shq1p around the Ser63 pocket is not well conserved, but serines elsewhere in the sequence might be targeted for phosphorylation in other species (Figure 1B) or this phosphorylation event may be specific for *S. cerevisiae*. Nevertheless, our observation of *in vitro* phosphorylation raises the question of whether Shq1p is phosphorylated *in vivo*. Preliminary studies show that *in vivo* Shq1p is phosphorylated (data not shown). However, since we have shown both the N- and C-terminal domains are phosphorylated by CK1 *in vitro* further work is underway to characterize which residues are phorphorylated *in vivo* and the impact of their phosphorylation on H/ACA snoRNP assembly *in vivo*.

Surprisingly, we found that Shq1p has stand-alone chaperone activity contained mainly by the Shq1p C-terminal domain but enhanced by the N-terminal domain. Enhancement of the chaperone activity requires both domains to be present in the same polypeptide. Similarly, Shq1p binds to Cbf5p primarily through its C-terminal domain, but the interaction is most clearly seen with the full length protein. Thus, Shq1p appears to identify potential client proteins and act as a chaperone on them primarily using the C-terminal domain, yet the two domains act in synergy to provide optimal activity. These properties were also observed with p23, where its flexible 50 amino acid C-terminal tail is necessary for identifying Hsp90 client-proteins and for inherent p23 chaperone activity[45]. Thus, Shq1p may act as a snoRNP-specific chaperone independently of Hsp90, or it may also assist the chaperone activity of Hsp90 by identifying Cbf5p as a client protein. The identification of Cbf5p as a potential Shq1p target is significant because all proteins and the RNA components of H/ACA particles contact Cbf5p, placing Shq1p at the heart of the complex biogenesis of this class of snoRNPs.

Conclusions

Our studies demonstrate that Shq1p is capable of Cbf5p recognition and that it has chaperone activity independent of its interaction with the yeast Hsp90 chaperone, suggesting that it may participate in chaperone-assisted maintenance or assembly of the H/ACA snoRNP. Since Shq1p does not interact efficiently with mature H/ACA particles, the interaction with Cbf5p occurs transiently during RNP assembly. The potential phosphorylation sites in both the N- and C-terminal domains suggest that the activity of Shq1p may be regulated by phosphorylation/dephosporylation to promote a specific chaperone activity, protein interaction, or subcellular localization. For example, Shq1p might be involved in the initial folding of Cbf5p or in the remodeling of H/ACA snoRNP that is required for maturation or subnuclear trafficking, and in stabilizing and destabilizing transient complexes during the maturation of the particle. *In vivo* experiments to dissect the function of Shq1p have been focused on the N-terminal domain and have been inconclusive. Our results clearly demonstrate that the C-terminal domain of Shq1p has identifiable biochemical activity. Its analysis will be necessary to understand when and how this protein functions as a chaperone or remodeling factor during H/ACA snoRNP biogenesis.

Materials and Methods

Plasmids

Full length Shq1p (Shq1FL), the N-terminal domain consisting of residues Ile2-Asn134 (Shq1Np), and the C-terminal domain (Shq1C) from Ile123-Gln507 were amplified by PCR from single yeast colonies of the CRY1 strain and cloned into pET32 (Novagen) using ligation independent cloning (LIC) techniques. All pET32-Shq1p constructs contain an N-terminal thioredoxin fusion protein and a 6xHis tag followed by a TEV protease cleavage site. Cbf5$^{\Delta}$p was PCR amplified from yeast as previously described[50] and cloned into pET28 with an N-terminal 6xHis tag. Hsp82p (yeast Hsp90) was also PCR amplified from yeast and cloned in pET30 by LIC techniques. Mutations were introduced using standard site directed mutagenesis.

Expression, purification, and proteolysis

Expression and purification of Cbf5$^{\Delta}$p and Hsp82p constructs was executed following previously reported protocols[31, 50]. Shq1p constructs were transformed into the *E. coli* Rosetta expression strain (Novagen) and grown at 37°C, induced with 0.2mM IPTG at 0.6 OD_{600}, and expressed for 10 hours at 30°C. For NMR, isotopic labeling was achieved by growth in M9 minimal media containing [^{15}N] NH_4Cl and [13C] glucose. Cell cultures were harvested by centrifugation at 6,000rpm 4°C for 10 minutes and lysed by sonication in buffer A (400mM KCl, 50mM potassium phosphate (pH 7.0), 4mM βME). The cleared lysate was applied to a

HisTrap nickel affinity column (Amersham) equilibrated in Buffer A and eluted with a linear gradient to Buffer B (Buffer A with 400mM Imidazole). Purified protein was then dialyzed into buffer C (200mM KCl, 50mM potassium phosphate (pH 7.0), 4mM β-mercaptoethanol) and digested with TEV protease containing a C-terminal 5xArg tag. In order to isolate the desired protein from the free 6xHis-tag and TEV protease, the digestion mixture was passed over another His-trap column equilibrated in buffer C before a final round of purification over a SD75 gel filtration column (Amersham) equilibrated in buffer C. For NMR studies, the proteins were dialyzed into 50mM KCl, 50mM potassium phosphate (pH 7.0), 4mM DTT.

The individual domains of Shq1p were identified after digesting the full-length protein with proteinase K, chymotrypsin, or trypsin according to the manufacturer's directions. The sequence identity of the C-terminal domain was verified by N-terminal protein sequencing by the Protein and Nucleic Acid facility at the Medical College of Wisconsin.

NMR Spectroscopy and Resonance Assignment

All NMR spectra collected for structure determination were performed at a protein concentration of 1.0mM and were recorded at 298K (unless otherwise stated). Triple resonance and HCCH-TOCSY[51] were recorded on a Bruker Avance 500 MHz spectrometer. 3D ^{15}N-edited NOESY and 3D ^{13}C-edited NOESY[52] were recorded at the Environmental Molecular Sciences Laboratory (EMSL) at the Pacific Northwest National Laboratory (PNNL) on a Varian INOVA 800 MHz and a Varian INOVA 600 MHz with cryoprobe, respectively.

Backbone resonance assignments of H, N, C^{α}, C′, and side-chain C^{β}were done using Triple resonance HNCA[53, 54], HNCO[54, 55], CBCA(CO)NH[56, 57], HNCACB, HBHACONH, and HN(CO)CA. The remaining side-chain resonance assignments were obtained from the analysis of ^{15}N-edited NOESY, ^{13}C-edited NOESY, and HCCH-TOCSY spectra. Aromatic ring protons and protected amides were identified from 2D ^{1}H,^{1}H-NOESY, ^{1}H,^{1}H-TOCSY and ^{15}N-HSQC, respectively, collected from a sample exchanged into a 100% $^{2}H_2O$ NMR buffer. Spectral data were processed using NMRPipe[58] and analyzed using Sparky[59].

Structure determination

Structure calculations were based on NOE cross-peaks identified from 3D ^{15}N- and ^{13}C-edited NOESYs and from a 2D ^{1}H, ^{1}H-NOESY recorded in 100% $^{2}H_2O$. CYANA 2.1[60, 61] was implemented for the semi-automated assignment of NOE cross-peaks based upon the chemical shifts generated from backbone and side-chain resonance assignments. Structure calculations were performed with the CALC algorithm implementing torsion angle dynamics and undergoing 8 cycles of iterative structure calculations. After the first rounds of calculations, the resulting structures and NOESY assignments were reviewed to remove artifact peaks, correct input backbone and side-chain assignments, to incorporate additional NOEs to improve regions of poor structural quality and to correct misidentified NOEs to be consistent with generated structural models. In order to satisfy the criteria for convergence defined by Herrmann et al.[62], additional constraints from torsion angle (φ/ϕ) values derived by TALOS[63] and hydrogen bonds were included in later rounds of refinement. Identification of the secondary structure elements was supported by the Chemical Shift Index (CSI) analysis[64]. The final CYANA 2.1 refinement cycle generated 20 conformers with the lowest target function, violations, and RMSD values of all calculations (Table 1). The final structures were validated using PROCHECK-NMR[65] (Table 1). Structural homologues were found through the DALI server[66] and figures were generated with MOLMOL[67]. The structure and experimental data were deposited with the PDB and BMRB.

ATP phosphorylation

Shq1p constructs were assayed for phosphorylation by incubating ~3ug of each protein with 0.5ug human Casein Kinase 1δor Casein Kinase 1ε(generously donated by Dr David Kimelman) in buffer D supplemented with 200uM ATP and 25nM ^{32}P-[γ]ATP (3000Ci/mmol) at 30°C for 1hr. For control kinase reactions, the same conditions were used for Protein Kinase A and Casein Kinase II. The reactions were stopped by addition of SDS loading dye, separated with 12.5% SDS-PAGE gel, dried and exposed overnight. The gels were imaged by autoradiography and analyzed using ImageQuant Molecular Dynamics software.

Citrate Synthase Aggregation Assay

Porcine heart citrate synthase (Roche Applied Science) at 0.4 μM final concentration was incubated with different amounts of Shq1FLp in 40 mM HEPES pH 7.5, 20 mM KOH, 50 mM KCl, 10 mM $(NH_4)_2SO_4$, and 2 mM CH_3COOK. Shq1Np and/or Shq1Cp or bovine serum albumin (BSA, New England Biolabs) were used instead of Shq1FLp in some assays. Samples (100 μL) were transferred to the thermostated cell of a Varian Eclipse fluorescence spectrophotometer and held at 45°C. Right angle light scattering was monitored for 15 min with the following settings: $\lambda_{EX/EM}$ = 500 nm, $slit_{EX/EM}$ = 2.5 nm. Control experiments were performed with each protein alone under the same conditions.

Cbf5p and Hsp90 interaction assay

Refolded Cbf5$^{\Delta}$(3.2nmol) was incubated with 40μL Ni-agarose beads (Qiagen) in buffer PD (200mM KCl, 20mM Tris-HCl (pH 8.0), 2mM βME, 0.2% Triton) at 4°C. After 1 hour, Cbf5$^{\Delta}$p was pulled down, washed 3 times with 200μL of buffer PD, and resuspended in PD buffer containing 2–3 times molar excess of Shq1FL, Shq1Np, or Shq1Cp and incubated at 4° C for an additional hour. The mixture was pulled down and washed with buffer PD as previously stated and eluted with 400mM imidazole. The eluate was analyzed by SDS-PAGE and Coomassie Brilliant Blue staining. The pull-down assay with Hsp82p, the yeast Hsp90 homologue, was conducted in the same manner as just described for the Cbf5p interaction. Before incubation with Ni-agarose beads, full length Hsp82p or the different Hsp90 constructs were activated by a 30 min pre-warming step at 30°C both in the presence or absence of 10-fold molar excess of ATP or ATP analogs. Sba1p, the yeast p23 homologue, was used as a positive control.

Accession Numbers

Coordinates and structure factors have been deposited in the Protein Data Bank with accession number 2K8Q

Supplementary Material

Refer to Web version on PubMed Central for supplementary material.

Acknowledgments

We would like to thank Drs. Per Widlund and Trisha Davis for supplying yeast cultures and the initial PCR amplification of Shq1p. We thank Dr. David Waugh for supplying a TEV protease expression line, Drs. Lina Dahlberg and David Kimelman for CK1ε, Philippe Meyer for Hsp82p constructs and Michael Pereckas of the Protein and Nucleic Acid Facility at the Medical College of Wisconsin for performing the N-terminal sequencing. NMR experiments collected at the Pacific Northwest National Laboratory were collected with the generous help of Nancy Isern and Dr. Tom Leeper and HetNOE data collection at the University of Washington was kindly performed by Brad Lunde. Work at the University of Washington was supported by NIH-NIGMS. Work at Université Paris-Sud was supported by the European 3D-repertoire program (LSHG-CT-2005-512028) and BIORIB grant (BLAN07-1_194553) from the Agence Nationale de la Recherche (ANR Blanche).

References

1. Meier UT. The many facets of H/ACA ribonucleoproteins. Chromosoma 2005;114:1–14. [PubMed: 15770508]
2. Maxwell ES, Fournier MJ. The small nucleolar RNAs. Annu Rev Biochem 1995;64:897–934. [PubMed: 7574504]
3. Ni J, Tien AL, Fournier MJ. Small nucleolar RNAs direct site-specific synthesis of pseudouridine in ribosomal RNA. Cell 1997;89:565–73. [PubMed: 9160748]
4. Ganot P, Bortolin ML, Kiss T. Site-specific pseudouridine formation in preribosomal RNA is guided by small nucleolar RNAs. Cell 1997;89:799–809. [PubMed: 9182768]
5. Darzacq X, Jady BE, Verheggen C, Kiss AM, Bertrand E, Kiss T. Cajal body-specific small nuclear RNAs: a novel class of 2′-O-methylation and pseudouridylation guide RNAs. Embo J 2002;21:2746–56. [PubMed: 12032087]
6. Richard P, Darzacq X, Bertrand E, Jady BE, Verheggen C, Kiss T. A common sequence motif determines the Cajal body-specific localization of box H/ACA scaRNAs. Embo J 2003;22:4283–93. [PubMed: 12912925]
7. Atzorn V, Fragapane P, Kiss T. U17/snR30 is a ubiquitous snoRNA with two conserved sequence motifs essential for 18S rRNA production. Mol Cell Biol 2004;24:1769–78. [PubMed: 14749391]
8. Morrissey JP, Tollervey D. U14 small nucleolar RNA makes multiple contacts with the pre-ribosomal RNA. Chromosoma 1997;105:515–22. [PubMed: 9211979]
9. Jady BE, Bertrand E, Kiss T. Human telomerase RNA and box H/ACA scaRNAs share a common Cajal body-specific localization signal. J Cell Biol 2004;164:647–52. [PubMed: 14981093]
10. Dez C, Henras A, Faucon B, Lafontaine D, Caizergues-Ferrer M, Henry Y. Stable expression in yeast of the mature form of human telomerase RNA depends on its association with the box H/ACA small nucleolar RNP proteins Cbf5p, Nhp2p and Nop10p. Nucleic Acids Res 2001;29:598–603. [PubMed: 11160879]
11. Mitchell JR, Cheng J, Collins K. A box H/ACA small nucleolar RNA-like domain at the human telomerase RNA 3′ end. Mol Cell Biol 1999;19:567–76. [PubMed: 9858580]
12. Lukowiak AA, Narayanan A, Li ZH, Terns RM, Terns MP. The snoRNA domain of vertebrate telomerase RNA functions to localize the RNA within the nucleus. Rna 2001;7:1833–44. [PubMed: 11780638]
13. Li H. Unveiling substrate RNA binding to H/ACA RNPs: one side fits all. Curr Opin Struct Biol 2008;18:78–85. [PubMed: 18178425]
14. Matera AG, Terns RM, Terns MP. Non-coding RNAs: lessons from the small nuclear and small nucleolar RNAs. Nat Rev Mol Cell Biol 2007;8:209–20. [PubMed: 17318225]
15. Darzacq X, Kittur N, Roy S, Shav-Tal Y, Singer RH, Meier UT. Stepwise RNP assembly at the site of H/ACA RNA transcription in human cells. J Cell Biol 2006;173:207–18. [PubMed: 16618814]
16. Kittur N, Darzacq X, Roy S, Singer RH, Meier UT. Dynamic association and localization of human H/ACA RNP proteins. Rna 2006;12:2057–62. [PubMed: 17135485]
17. Ballarino M, Morlando M, Pagano F, Fatica A, Bozzoni I. The cotranscriptional assembly of snoRNPs controls the biosynthesis of H/ACA snoRNAs in Saccharomyces cerevisiae. Mol Cell Biol 2005;25:5396–403. [PubMed: 15964797]
18. Yang PK, Hoareau C, Froment C, Monsarrat B, Henry Y, Chanfreau G. Cotranscriptional recruitment of the pseudouridylsynthetase Cbf5p and of the RNA binding protein Naf1p during H/ACA snoRNP assembly. Mol Cell Biol 2005;25:3295–304. [PubMed: 15798213]
19. Girard JP, Lehtonen H, Caizergues-Ferrer M, Amalric F, Tollervey D, Lapeyre B. GAR1 is an essential small nucleolar RNP protein required for pre-rRNA processing in yeast. Embo J 1992;11:673–82. [PubMed: 1531632]
20. Pellizzoni LBJ, Charroux B, Dreyfuss G. The survival of motor neurons (SMN) protein interacts with the snoRNP proteins fibrillarin and GAR1. Curr Biol 2001;11:1079–1088. [PubMed: 11509230]
21. Leulliot N, Godin KS, Hoareau-Aveilla C, Quevillon-Cheruel S, Varani G, Henry Y, Van Tilbeurgh H. The box H/ACA RNP assembly factor Naf1p contains a domain homologous to Gar1p mediating its interaction with Cbf5p. J Mol Biol 2007;371:1338–53. [PubMed: 17612558]

22. Yang PK, Rotondo G, Porras T, Legrain P, Chanfreau G. The Shq1p. Naf1p complex is required for box H/ACA small nucleolar ribonucleoprotein particle biogenesis. J Biol Chem 2002;277:45235–42. [PubMed: 12228251]
23. Ho Y, Gruhler A, Heilbut A, Bader GD, Moore L, Adams SL, Millar A, Taylor P, Bennett K, Boutilier K, Yang L, Wolting C, Donaldson I, Schandorff S, Shewnarane J, Vo M, Taggart J, Goudreault M, Muskat B, Alfarano C, Dewar D, Lin Z, Michalickova K, Willems AR, Sassi H, Nielsen PA, Rasmussen KJ, Andersen JR, Johansen LE, Hansen LH, Jespersen H, Podtelejnikov A, Nielsen E, Crawford J, Poulsen V, Sorensen BD, Matthiesen J, Hendrickson RC, Gleeson F, Pawson T, Moran MF, Durocher D, Mann M, Hogue CW, Figeys D, Tyers M. Systematic identification of protein complexes in Saccharomyces cerevisiae by mass spectrometry. Nature 2002;415:180–3. [PubMed: 11805837]
24. Singh M, Gonzales FA, Cascio D, Heckmann N, Chanfreau G, Feigon J. Structure and functional studies of the CS domain of the essential H/ACA RNP assembly protein Shq1. J Biol Chem. 2008
25. Mulder N, Apweiler R. InterPro and InterProScan: tools for protein sequence classification and comparison. Methods Mol Biol 2007;396:59–70. [PubMed: 18025686]
26. Grozdanov PN, Roy S, Kittur N, Meier UT. SHQ1 is required prior to NAF1 for assembly of H/ACA small nucleolar and telomerase RNPs. Rna. 2009
27. Holm L, Kaariainen S, Rosenstrom P, Schenkel A. Searching protein structure databases with DaliLite v.3. Bioinformatics. 2008
28. Stamler R, Kappe G, Boelens W, Slingsby C. Wrapping the alpha-crystallin domain fold in a chaperone assembly. J Mol Biol 2005;353:68–79. [PubMed: 16165157]
29. Buchner J, Weikl T, Bugl H, Pirkl F, Bose S. Purification of Hsp90 partner proteins Hop/p60, p23, and FKBP52. Methods Enzymol 1998;290:418–29. [PubMed: 9534179]
30. Takahashi A, Casais C, Ichimura K, Shirasu K. HSP90 interacts with RAR1 and SGT1 and is essential for RPS2-mediated disease resistance in Arabidopsis. Proc Natl Acad Sci U S A 2003;100:11777–82. [PubMed: 14504384]
31. Ali MM, Roe SM, Vaughan CK, Meyer P, Panaretou B, Piper PW, Prodromou C, Pearl LH. Crystal structure of an Hsp90-nucleotide-p23/Sba1 closed chaperone complex. Nature 2006;440:1013–7. [PubMed: 16625188]
32. Kadota Y, Amigues B, Ducassou L, Madaoui H, Ochsenbein F, Guerois R, Shirasu K. Structural and functional analysis of SGT1-HSP90 core complex required for innate immunity in plants. EMBO Rep. 2008
33. Zhang M, Boter M, Li K, Kadota Y, Panaretou B, Prodromou C, Shirasu K, Pearl LH. Structural and functional coupling of Hsp90- and Sgt1-centred multi-protein complexes. Embo J 2008;27:2789–98. [PubMed: 18818696]
34. Lee YT, Jacob J, Michowski W, Nowotny M, Kuznicki J, Chazin WJ. Human Sgt1 binds HSP90 through the CHORD-Sgt1 domain and not the tetratricopeptide repeat domain. J Biol Chem 2004;279:16511–7. [PubMed: 14761955]
35. da Silva Correia J, Miranda Y, Leonard N, Ulevitch R. SGT1 is essential for Nod1 activation. Proc Natl Acad Sci U S A 2007;104:6764–9. [PubMed: 17420470]
36. Lingelbach LB, Kaplan KB. The interaction between Sgt1p and Skp1p is regulated by HSP90 chaperones and is required for proper CBF3 assembly. Mol Cell Biol 2004;24:8938–50. [PubMed: 15456868]
37. Catlett MG, Kaplan KB. Sgt1p is a unique co-chaperone that acts as a client adaptor to link Hsp90 to Skp1p. J Biol Chem 2006;281:33739–48. [PubMed: 16945921]
38. Wong YH, Lee TY, Liang HK, Huang CM, Wang TY, Yang YH, Chu CH, Huang HD, Ko MT, Hwang JK. KinasePhos 2.0: a web server for identifying protein kinase-specific phosphorylation sites based on sequences and coupling patterns. Nucleic Acids Res 2007;35:W588–94. [PubMed: 17517770]
39. Knippschild U, Wolff S, Giamas G, Brockschmidt C, Wittau M, Wurl PU, Eismann T, Stoter M. The role of the casein kinase 1 (CK1) family in different signaling pathways linked to cancer development. Onkologie 2005;28:508–14. [PubMed: 16186692]

40. Ferrarese A, Marin O, Bustos VH, Venerando A, Antonelli M, Allende JE, Pinna LA. Chemical dissection of the APC Repeat 3 multistep phosphorylation by the concerted action of protein kinases CK1 and GSK3. Biochemistry 2007;46:11902–10. [PubMed: 17910481]
41. Gross S, Moore CL. Rna15 interaction with the A-rich yeast polyadenylation signal is an essential step in mRNA 3′-end formation. Mol Cell Biol 2001;21:8045–55. [PubMed: 11689695]
42. Knippschild U, Gocht A, Wolff S, Huber N, Lohler J, Stoter M. The casein kinase 1 family: participation in multiple cellular processes in eukaryotes. Cell Signal 2005;17:675–89. [PubMed: 15722192]
43. Muchowski PJ, Clark JI. ATP-enhanced molecular chaperone functions of the small heat shock protein human alphaB crystallin. Proc Natl Acad Sci U S A 1998;95:1004–9. [PubMed: 9448275]
44. Bose S, Weikl T, Bugl H, Buchner J. Chaperone function of Hsp90-associated proteins. Science 1996;274:1715–7. [PubMed: 8939863]
45. Weaver AJ, Sullivan WP, Felts SJ, Owen BA, Toft DO. Crystal structure and activity of human p23, a heat shock protein 90 co-chaperone. J Biol Chem 2000;275:23045–52. [PubMed: 10811660]
46. Boulon S, Marmier-Gourrier N, Pradet-Balade B, Wurth L, Verheggen C, Jady BE, Rothe B, Pescia C, Robert MC, Kiss T, Bardoni B, Krol A, Branlant C, Allmang C, Bertrand E, Charpentier B. The Hsp90 chaperone controls the biogenesis of L7Ae RNPs through conserved machinery. J Cell Biol 2008;180:579–95. [PubMed: 18268104]
47. Zhao R, Kakihara Y, Gribun A, Huen J, Yang G, Khanna M, Costanzo M, Brost RL, Boone C, Hughes TR, Yip CM, Houry WA. Molecular chaperone Hsp90 stabilizes Pih1/Nop17 to maintain R2TP complex activity that regulates snoRNA accumulation. J Cell Biol 2008;180:563–78. [PubMed: 18268103]
48. Krogan NJ, Cagney G, Yu H, Zhong G, Guo X, Ignatchenko A, Li J, Pu S, Datta N, Tikuisis AP, Punna T, Peregrin-Alvarez JM, Shales M, Zhang X, Davey M, Robinson MD, Paccanaro A, Bray JE, Sheung A, Beattie B, Richards DP, Canadien V, Lalev A, Mena F, Wong P, Starostine A, Canete MM, Vlasblom J, Wu S, Orsi C, Collins SR, Chandran S, Haw R, Rilstone JJ, Gandi K, Thompson NJ, Musso G, St Onge P, Ghanny S, Lam MH, Butland G, Altaf-Ul AM, Kanaya S, Shilatifard A, O'Shea E, Weissman JS, Ingles CJ, Hughes TR, Parkinson J, Gerstein M, Wodak SJ, Emili A, Greenblatt JF. Global landscape of protein complexes in the yeast Saccharomyces cerevisiae. Nature 2006;440:637–43. [PubMed: 16554755]
49. Zhao R, Davey M, Hsu YC, Kaplanek P, Tong A, Parsons AB, Krogan N, Cagney G, Mai D, Greenblatt J, Boone C, Emili A, Houry WA. Navigating the chaperone network: an integrative map of physical and genetic interactions mediated by the hsp90 chaperone. Cell 2005;120:715–27. [PubMed: 15766533]
50. Normand C, Capeyrou R, Quevillon-Cheruel S, Mougin A, Henry Y, Caizergues-Ferrer M. Analysis of the binding of the N-terminal conserved domain of yeast Cbf5p to a box H/ACA snoRNA. Rna 2006;12:1868–82. [PubMed: 16931875]
51. Kay LEXGY, Singer AU, Muhandiram DR, Formankay JD. A Gradient-Enhanced HCCH-TOCSY Experiment for Recording Side-Chain 1H and 13C Correlations in H2O Samples of Proteins. Journal of Magnetic Resonance, Series B 1993;101:333–337.
52. Muhandiram DRFNA, Xu GY, Smallcombe SH, Kay LE. A Gradient 13C NOESY-HSQC Experiment for Recording NOESY Spectra of 13C-Labeled Proteins Dissolved in H2O. Journal of Magnetic Resonance, Series B 1993;102:317–321.
53. Yamazaki T, Lee Weontae, Revington Matthew, Mattiello Debra L, Dahlquist Frederick W, Arrowsmith Cheryl H, Kay Lewis E. An HNCA Pulse Scheme for the Backbone Assignment of 15N, 13C,2H-Labeled Proteins: Application to a 37-kDa Trp Repressor-DNA Complex. J Am Chem Soc 1994;116:6464–6465.
54. Mori SAC, Johnson MO, Vanzijl PCM. Improved Sensitivity of HSQC Spectra of Exchanging Protons at Short Interscan Delays Using a New Fast HSQC (FHSQC) Detection Scheme That Avoids Water Saturation. Journal of Magnetic Resonance, Series B 1995;108:94–98. [PubMed: 7627436]
55. Kay LEXGY, Yamazaki T. Enhanced-Sensitivity Triple-Resonance Spectroscopy with Minimal H2O Saturation. Journal of Magnetic Resonance, Series A 1994;109:129–133.
56. Grzesiek, SaBAd. Correlating backbone amide and side chain resonances in larger proteins by multiple relayed triple resonance NMR. J Am Chem Soc 1992;114:6291–6293.

57. Muhandiram DRKLE. Gradient-Enhanced Triple-Resonance Three-Dimensional NMR Experiments with Improved Sensitivity. Journal of Magnetic Resonance, Series B 1994;103:203–216.
58. Delaglio F, Grzesiek S, Vuister GW, Zhu G, Pfeifer J, Bax A. NMRPipe: a multidimensional spectral processing system based on UNIX pipes. J Biomol NMR 1995;6:277–93. [PubMed: 8520220]
59. Goddard, TD.; Kneller, DG. SPARKY 3. University of California; San Francisco:
60. Herrmann T, Guntert P, Wuthrich K. Protein NMR structure determination with automated NOE-identification in the NOESY spectra using the new software ATNOS. J Biomol NMR 2002;24:171–89. [PubMed: 12522306]
61. Guntert P, Mumenthaler C, Wuthrich K. Torsion angle dynamics for NMR structure calculation with the new program DYANA. J Mol Biol 1997;273:283–98. [PubMed: 9367762]
62. Herrmann T, Guntert P, Wuthrich K. Protein NMR structure determination with automated NOE assignment using the new software CANDID and the torsion angle dynamics algorithm DYANA. J Mol Biol 2002;319:209–27. [PubMed: 12051947]
63. Cornilescu G, Delaglio F, Bax A. Protein backbone angle restraints from searching a database for chemical shift and sequence homology. J Biomol NMR 1999;13:289–302. [PubMed: 10212987]
64. Wishart DS, Sykes BD. The 13C chemical-shift index: a simple method for the identification of protein secondary structure using 13C chemical-shift data. J Biomol NMR 1994;4:171–80. [PubMed: 8019132]
65. Laskowski RA, Rullmannn JA, MacArthur MW, Kaptein R, Thornton JM. AQUA and PROCHECK-NMR: programs for checking the quality of protein structures solved by NMR. J Biomol NMR 1996;8:477–86. [PubMed: 9008363]
66. Holm L, Sander C. Dali/FSSP classification of three-dimensional protein folds. Nucleic Acids Res 1997;25:231–4. [PubMed: 9016542]
67. Koradi R, Billeter M, Wuthrich K. MOLMOL: a program for display and analysis of macromolecular structures. J Mol Graph 1996;14:51–5. 29–32. [PubMed: 8744573]

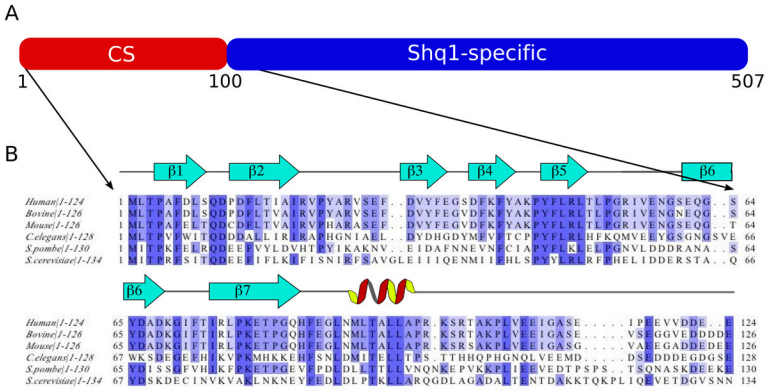

Figure 1. Conservation of Shq1p in eukaryotes

A) Cartoon representation of the Shq1p domain organization. B) Sequence alignment of the Shq1p N-terminus (Shq1Np) from yeast to humans showing the secondary structural elements as identified by NMR. Identical residues are indicated in blue; the darkest blue represents 100% conservation.

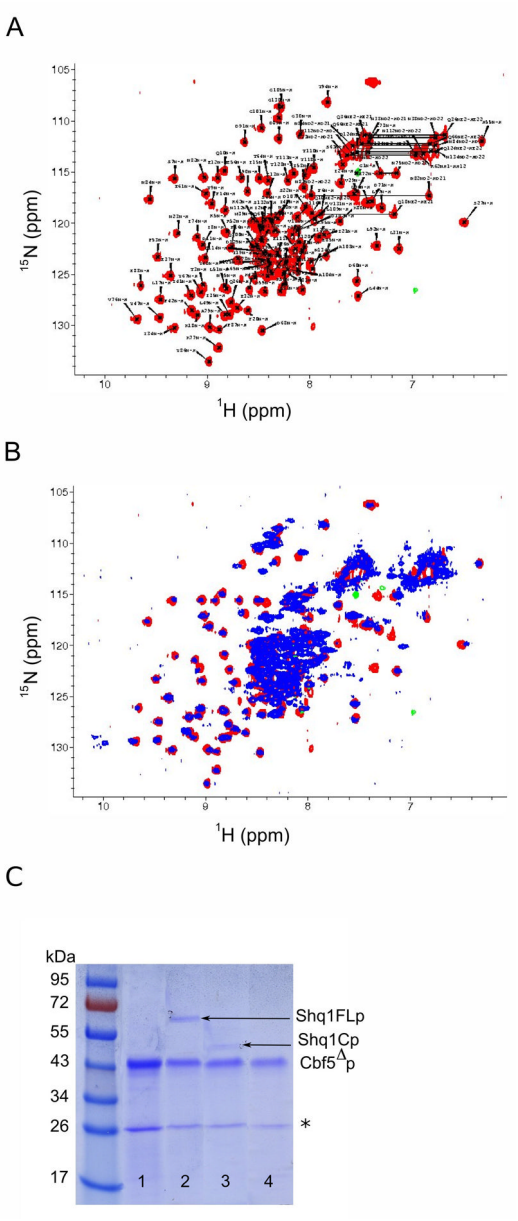

Figure 2. Assessment of Shq1p domain structure by ^{15}N-HSQC

A) ^{15}N-labeled HSQC of Shq1Np 50mM KCl, 50mM potassium phosphate (pH 7.0), and 4mM DTT. B) ^{15}N-HSQC of Shq1FLp in 200mM KCl, 50mM potassium phosphate (pH 7.0), and 4mM DTT overlayed with the ^{15}N-HSQC of Shq1Np shown in part A. Both spectra were recorded at 298K on a Bruker Avance 500MHz spectrometer. C) Shq1p interacts with Cbf5p *in vitro*. Refolded Cbf5$^{\Delta}$p bound to Ni-agarose beads (lane 1) was treated with 3-fold molar excess of each Shq1p construct. SDS-PAGE analysis of each elution shows that full length Shq1p (lane 2) associates with Cbf5$^{\Delta}$p while Shq1Cp (lane 3) is only weakly bound and Shq1Np (lane 4) is not apparently binding to Cbf5$^{\Delta}$p under these conditions. The far left well shows the molecular weight marker and the asterisk marks a Cbf5$^{\Delta}$p degradation product.

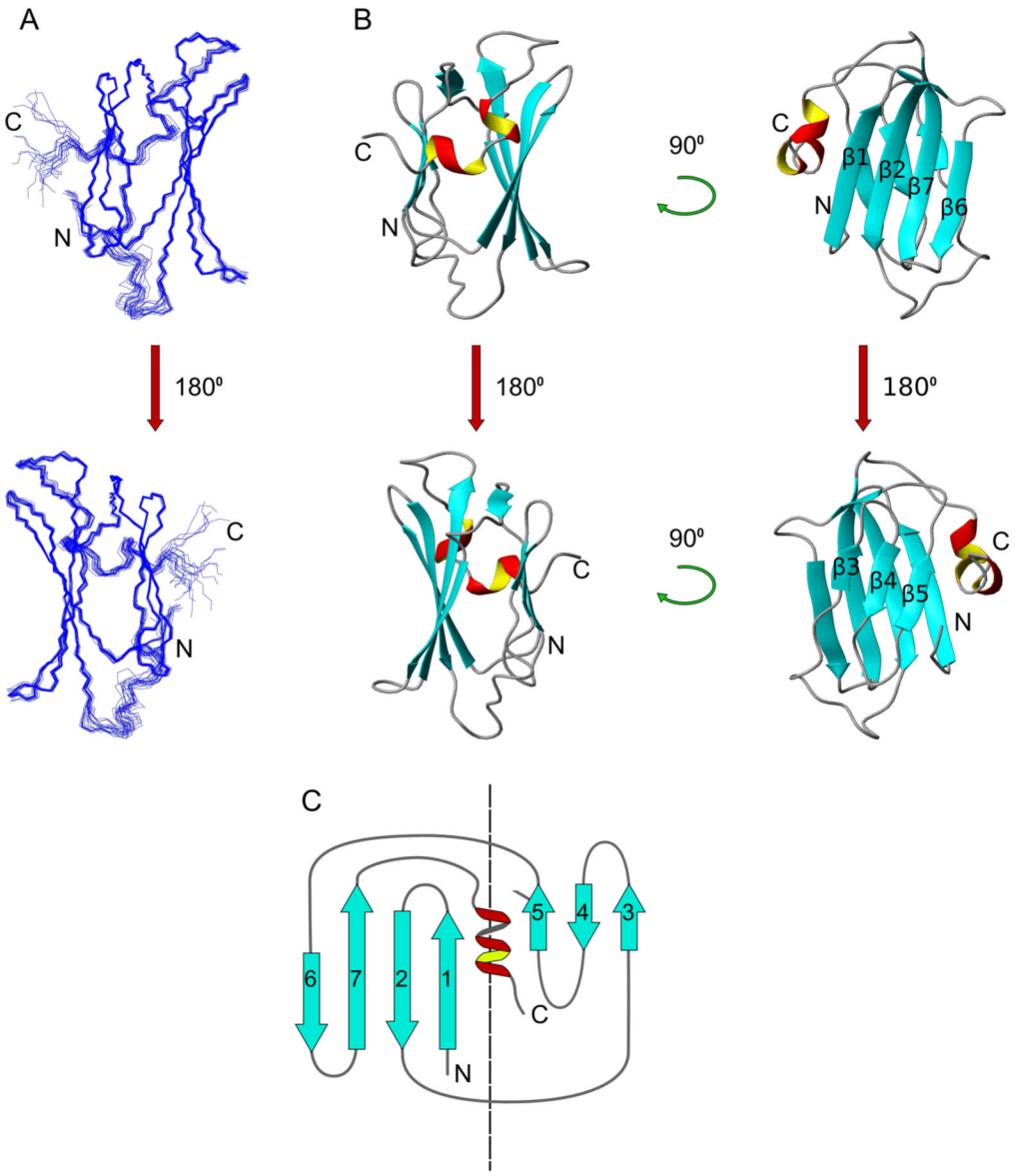

Figure 3. Solution structure of the Shq1p CS domain

A) Backbone trace of 20 structures calculated with CYANA-2.1 having the lowest target function and violations. The structures agree to within ~0.20A r.m.s.d. of the mean, when calculated over the structured regions. B) Cartoon representation showing each face of the Shq1Np CS domain β-sandwich. C) Structural topology of Shq1Np.

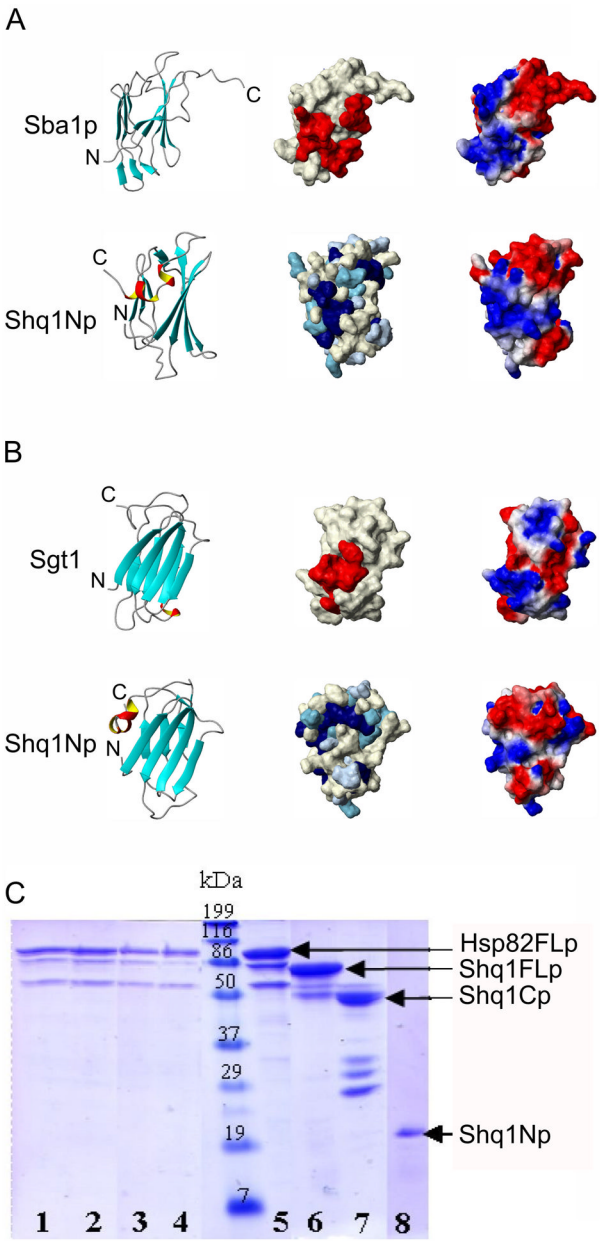

Figure 4. Comparison of Shq1Np with Hsp90 co-chaperones

Shq1Np (bottom views) is compared with the Hsp90 binding interface of A) *S. cereviseae* Sba1p (2CG9) and B) *A. thaliana* Sgt1 (2JK1). Sba1p and Sgt1 use distinct modes of Hsp90 recognition and each are shown along their Hsp90 binding interfaces. In each panel, Shq1Np is shown in the orientation that corresponds with either the Hsp90 binding interface of Sba1p in A) or that of Sgt1 in B). In the left panel, each protein is shown as a ribbon representation. Shq1Np shares the same β-sheet organization with both co-chaperones, but contains a C-terminal helix where Sgt1 lacks structure beyond the β-sandwich and Sba1 instead has a β-strand that interacts with the N-terminal region of the 4-stranded β-sheet. In the middle panel, residues found at the Hsp90 interface of Sba1p and Sgt1 are shown in red and compared with highly conserved surface exposed residues of Shq1Np, which are colored according to the sequence alignment shown in Figure 1. In the right panel, the electrostatic surface potential

corresponding to the Hsp90 binding interface of Sba1p in A) and Sgt1 in B). The middle and right panel show that conserved residues on Shq1Np correspond with the interaction pattern observed for the Sba1p-Hsp90 interaction interface and that these two proteins are more similar to each other, with regards to electrostatic surface potential, than Shq1Np and Sgt1. C) Shq1p does not interact directly with Hsp82p, the yeast Hsp90 homologue, *in vitro*. Hsp82p bound to Ni-agarose beads in the presence of 10-fold molar excess of ATP (lane 1) was incubated with a 3-fold molar excess of each Shq1p construct. SDS-PAGE analysis of each elution shows that full length Shq1p (lane 2), Shq1Cp (lane 3) and Shq1Np (lane 4) do not bind to Hsp82p under these conditions. The middle well contains molecular weight marker. Lanes 5 to 8 show the migration profiles of each protein involved in the pull-down assay. The same results were obtained with Hsp82p without ATP or with ATP analogs (data not shown).

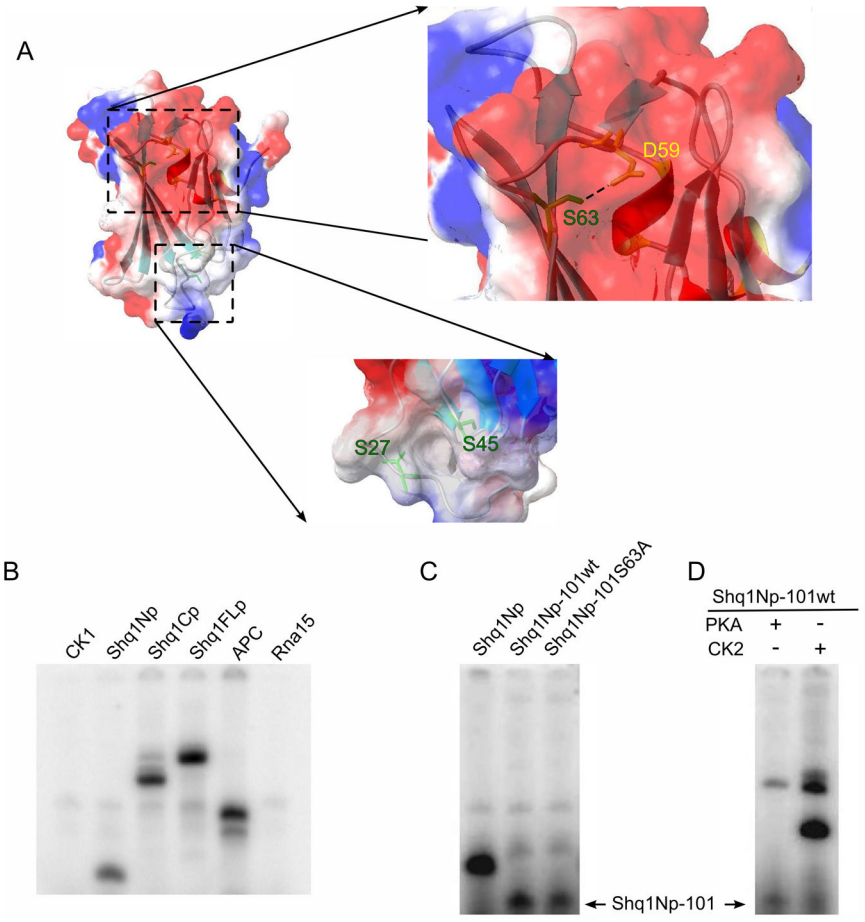

Figure 5. Shq1p is a phosphorylated protein

A) Shq1Np has two serine-containing pockets; one located in a region of negative electrostatic potential between strands β3 and β6 (top) and a second the between the β2–β3 and β4–β5 loops (bottom). The upper boxed region shows a closer look at residues within a CK1 consensus sequence specifically S63 (in green) that is within 3Å of D59 (in yellow). B) Incubation of full length Shq1p and its N- and C-terminal domains with CK1εin the presence of ^{32}P-[γ]ATP shows that γ-phosphate is transferred to all Shq1p constructs. The R3 region of APC is a known target of CK1 and was used as a positive control while Rna15p, a protein associated with 3′ end processing of RNAP II transcripts, was predicted to not contain a CK1 phosphorylation and showed no CK1 phosphorylation. C) Phosphorylation of Shq1Np, the G101 truncation mutation of Shq1Np, and the G101 truncation of the Shq1Np S63A mutation with CK1δ at 30°C for 30 minutes. D) Phosphorylation of Shq1Np-G101 with kinases PKA and CK2 at 30° C for 16hrs.

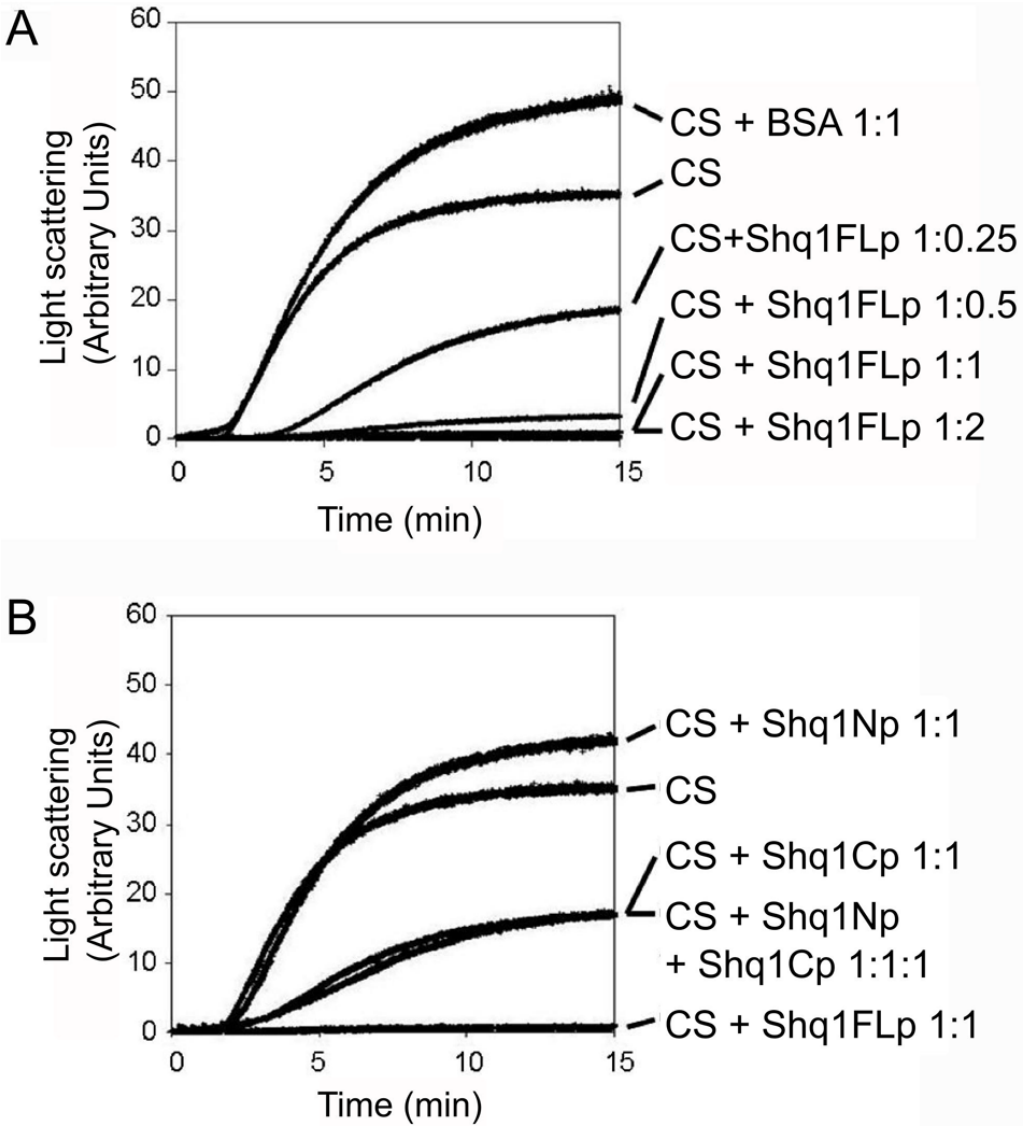

Figure 6. Shq1p has chaperone activity

(A) Aggregation of citrate synthase (CS) was followed by light scattering at 45°C without additives and in the presence of an equimolar ratio (based on monomers) of BSA, or with increasing molar ratios of full length Shq1. (B) Aggregation of citrate synthase at 45°C was measured by light scattering in the presence of equimolar ratios (based on monomers) of full length Shq1p, Shq1Np and/or Shq1Cp, or in the absence of additional proteins.

Table 1
Experimental restraints and structural statistics

	Shq1N
Structural Constraints	
Distance constraints[a]	
Total meaningful NOE restraints	2469
Short range (|I–j| = 1)	1326
Medium-range (|I–j| < 4)	304
Long-range (|I–j| > 5)	839
Hydrogen bond restraints	96
Saltbridge restraints	2
Dihedral angle restraints (ϕ,ψ)[b]	54
Total Number of Constraints	**2621**
Constraints per residue	~19.8
Residual Constraint Violations[c]	
Cyana Target Function (Å^2)	1.57 +/− 0.0057
Distance violations (>0.2 Å)	0 (0.18)
Torsion angles (>5.0 Å)	0 (4.31)
Average RMSD to mean (Å)[d]	
Heavy atom	0.71 +/− 0.04
Backbone	0.25 +/− 0.05
Ramachandran Statistics (%)[e]	
Favored	78.4
Additionally allowed	20.5
Generously allowed	0.2
Disallowed	0.9

[a] Final 20/100 structures selected based on lowest CYANA target function

[b] Dihedral angle restraints derived from TALOS

[c] Maximum violation shown in parenthesis

[d] Average RMSD to mean calculated over regions of consistent structure.

[e] Ramachandran analysis was performed by PROCHECK NMR.